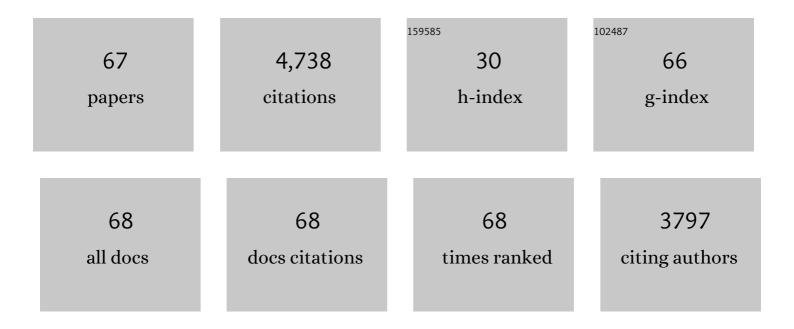
List of Publications by Year in descending order

Source: https://exaly.com/author-pdf/7507833/publications.pdf Version: 2024-02-01



#	Article	IF	CITATIONS
1	Functionalized polyarylether-based COFs for rapid and selective extraction of uranium from aqueous solution. Chemical Engineering Journal, 2022, 434, 134623.	12.7	46
2	Turn-up Luminescent Sensing of Ultraviolet Radiation by Lanthanide Metal–Organic Frameworks. Inorganic Chemistry, 2022, 61, 4561-4565.	4.0	10
3	Efficient Xe/Kr Separation Based on a Lanthanide–Organic Framework with One-Dimensional Local Positively Charged Rhomboid Channels. ACS Applied Materials & Interfaces, 2022, 14, 22233-22241.	8.0	18
4	<i>In Vivo</i> Uranium Decorporation by a Tailor-Made Hexadentate Ligand. Journal of the American Chemical Society, 2022, 144, 11054-11058.	13.7	28
5	The effects of fluorination and hydrogenation on the physical properties of two-dimensional (111)-oriented cubic boron nitride nanosheets. Thin Solid Films, 2021, 718, 138484.	1.8	2
6	Efficient Sr-90 removal from highly alkaline solution by an ultrastable crystalline zirconium phosphonate. Chemical Communications, 2021, 57, 8452-8455.	4.1	15
7	Unveiling the Uncommon Fluorescent Recognition Mechanism towards Pertechnetate Using a Cationic Metal–Organic Framework Bearing Nâ€Heterocyclic AIE Molecules. Chemistry - A European Journal, 2021, 27, 5632-5637.	3.3	19
8	A nitrogen-rich covalent organic framework for simultaneous dynamic capture of iodine and methyl iodide. CheM, 2021, 7, 699-714.	11.7	197
9	Deuterated Covalent Organic Frameworks with Significantly Enhanced Luminescence. Angewandte Chemie, 2021, 133, 21420-21425.	2.0	0
10	Deuterated Covalent Organic Frameworks with Significantly Enhanced Luminescence. Angewandte Chemie - International Edition, 2021, 60, 21250-21255.	13.8	30
11	Task-Specific Tailored Cationic Polymeric Network with High Base-Resistance for Unprecedented ⁹⁹ TcO ₄ [–] Cleanup from Alkaline Nuclear Waste. ACS Central Science, 2021, 7, 1441-1450.	11.3	101
12	Chromate separation by selective crystallization. Chinese Chemical Letters, 2020, 31, 1974-1977.	9.0	9
13	99TcO4â^' removal from legacy defense nuclear waste by an alkaline-stable 2D cationic metal organic framework. Nature Communications, 2020, 11, 5571.	12.8	124
14	Emergence of a Radicalâ€Stabilizing Metal–Organic Framework as a Radioâ€photoluminescence Dosimeter. Angewandte Chemie - International Edition, 2020, 59, 15209-15214.	13.8	56
15	Ab-Initio Study of the Electronic and Magnetic Properties of Boron- and Nitrogen-Doped Penta-Graphene. Nanomaterials, 2020, 10, 816.	4.1	11
16	A Porous Aromatic Framework Functionalized with Luminescent Iridium(III) Organometallic Complexes for Turn-On Sensing of ⁹⁹ TcO ₄ [–] . ACS Applied Materials & Interfaces, 2020, 12, 15288-15297.	8.0	46
17	Stabilization of Open-Shell Single Bonds within Endohedral Metallofullerene. Inorganic Chemistry, 2020, 59, 3606-3618.	4.0	11
18	Electron Beam Irradiation as a General Approach for the Rapid Synthesis of Covalent Organic Frameworks under Ambient Conditions. Journal of the American Chemical Society, 2020, 142, 9169-9174.	13.7	90

#	Article	IF	CITATIONS
19	Emergence of a Radicalâ€Stabilizing Metal–Organic Framework as a Radioâ€photoluminescence Dosimeter. Angewandte Chemie, 2020, 132, 15321-15326.	2.0	14
20	Stimulating antibacterial activities of graphitic carbon nitride nanosheets with plasma treatment. Nanoscale, 2019, 11, 18416-18425.	5.6	41
21	Inorganic X-ray Scintillators Based on a Previously Unnoticed but Intrinsically Advantageous Metal Center. Inorganic Chemistry, 2019, 58, 2807-2812.	4.0	13
22	A 3,2-Hydroxypyridinone-based Decorporation Agent that Removes Uranium from Bones In Vivo. Nature Communications, 2019, 10, 2570.	12.8	107
23	Powerful uranium extraction strategy with combined ligand complexation and photocatalytic reduction by postsynthetically modified photoactive metal-organic frameworks. Applied Catalysis B: Environmental, 2019, 254, 47-54.	20.2	222
24	Distinctive Two-Step Intercalation of Sr2+ into a Coordination Polymer with Record High 90Sr Uptake Capabilities. CheM, 2019, 5, 977-994.	11.7	119
25	Mechanism unravelling for ultrafast and selective ⁹⁹ TcO ₄ ^{â^'} uptake by a radiation-resistant cationic covalent organic framework: a combined radiological experiment and molecular dynamics simulation study. Chemical Science, 2019, 10, 4293-4305.	7.4	181
26	Successful Decontamination of ⁹⁹ TcO ₄ ^{â^'} in Groundwater at Legacy Nuclear Sites by a Cationic Metalâ€Organic Framework with Hydrophobic Pockets. Angewandte Chemie - International Edition, 2019, 58, 4968-4972.	13.8	177
27	Successful Decontamination of ⁹⁹ TcO ₄ ^{â^'} in Groundwater at Legacy Nuclear Sites by a Cationic Metalâ€Organic Framework with Hydrophobic Pockets. Angewandte Chemie, 2019, 131, 5022-5026.	2.0	37
28	Ratiometric Monitoring of Thorium Contamination in Natural Water Using a Dual-Emission Luminescent Europium Organic Framework. Environmental Science & Technology, 2019, 53, 332-341.	10.0	90
29	C–O ^{â^'} –K ⁺ (Na ⁺) groups in non-doped carbon as active sites for the oxygen reduction reaction. Journal of Materials Chemistry A, 2018, 6, 8955-8961.	10.3	28
30	Unique Proton Transportation Pathway in a Robust Inorganic Coordination Polymer Leading to Intrinsically High and Sustainable Anhydrous Proton Conductivity. Journal of the American Chemical Society, 2018, 140, 6146-6155.	13.7	181
31	Facile and Efficient Decontamination of Thorium from Rare Earths Based on Selective Selenite Crystallization. Inorganic Chemistry, 2018, 57, 1880-1887.	4.0	32
32	Phase transition triggered aggregation-induced emission in a photoluminescent uranyl–organic framework. Chemical Communications, 2018, 54, 627-630.	4.1	35
33	Highly Sensitive Detection of UV Radiation Using a Uranium Coordination Polymer. ACS Applied Materials & Interfaces, 2018, 10, 4844-4850.	8.0	52
34	An Ultrastable Heterobimetallic Uranium(IV)/Vanadium(III) Solid Compound Protected by a Redox-Active Phosphite Ligand: Crystal Structure, Oxidative Dissolution, and First-Principles Simulation. Inorganic Chemistry, 2018, 57, 903-907.	4.0	8
35	Palladium concave nanocrystals with high-index facets accelerate ascorbate oxidation in cancer treatment. Nature Communications, 2018, 9, 4861.	12.8	84
36	Degradable Carbon Dots with Broad-Spectrum Antibacterial Activity. ACS Applied Materials & Interfaces, 2018, 10, 26936-26946.	8.0	246

#	Article	IF	CITATIONS
37	99TcO4â^ remediation by a cationic polymeric network. Nature Communications, 2018, 9, 3007.	12.8	234
38	Highly Sensitive and Selective Uranium Detection in Natural Water Systems Using a Luminescent Mesoporous Metal–Organic Framework Equipped with Abundant Lewis Basic Sites: A Combined Batch, X-ray Absorption Spectroscopy, and First Principles Simulation Investigation. Environmental Science & Technology, 2017, 51, 3911-3921.	10.0	331
39	Exceptional Perrhenate/Pertechnetate Uptake and Subsequent Immobilization by a Low-Dimensional Cationic Coordination Polymer: Overcoming the Hofmeister Bias Selectivity. Environmental Science and Technology Letters, 2017, 4, 316-322.	8.7	181
40	Overcoming the crystallization and designability issues in the ultrastable zirconium phosphonate framework system. Nature Communications, 2017, 8, 15369.	12.8	366
41	ldentifying the Recognition Site for Selective Trapping of ⁹⁹ TcO ₄ [–] in a Hydrolytically Stable and Radiation Resistant Cationic Metal–Organic Framework. Journal of the American Chemical Society, 2017, 139, 14873-14876.	13.7	386
42	Hydroxyl-Group-Dominated Graphite Dots Reshape Laser Desorption/Ionization Mass Spectrometry for Small Biomolecular Analysis and Imaging. ACS Nano, 2017, 11, 9500-9513.	14.6	79
43	Thickness dependent semiconductor-to-metal transition of two-dimensional polyaniline with unique work functions. Nanoscale, 2017, 9, 12025-12031.	5.6	24
44	Electronic structural properties of BiOF crystal and its oxygen vacancy from first-principles calculations. Russian Journal of Physical Chemistry A, 2017, 91, 2425-2430.	0.6	3
45	A mesoporous cationic thorium-organic framework that rapidly traps anionic persistent organic pollutants. Nature Communications, 2017, 8, 1354.	12.8	296
46	The selfâ€consistent charge density functional tightâ€binding theory study of carbon adatoms using tuned Hubbard <i>U</i> parameters. International Journal of Quantum Chemistry, 2017, 117, e25320.	2.0	1
47	Self-Assembled Core–Satellite Gold Nanoparticle Networks for Ultrasensitive Detection of Chiral Molecules by Recognition Tunneling Current. ACS Nano, 2016, 10, 5096-5103.	14.6	47
48	Th(H2O)(IVO3)2[IVII0.6V1.76O7(OH)]: A Mixed-Valent Iodine Compound Containing Periodate Stabilized by Crystallographically Compatible Lattice Sites. Inorganic Chemistry, 2016, 55, 12101-12104.	4.0	7
49	Depolymerization of Freeâ€Radical Polymers with Spin Migrations. ChemPhysChem, 2015, 16, 3308-3312.	2.1	11
50	A strong charge-transfer effect in surface-enhanced Raman scattering induced by valence electrons of actinide elements. RSC Advances, 2015, 5, 32198-32204.	3.6	23
51	Electronic delocalization in small water rings. Physical Chemistry Chemical Physics, 2015, 17, 2987-2990.	2.8	18
52	Correlation between electron delocalization and structural planarization in small water rings. International Journal of Quantum Chemistry, 2015, 115, 817-819.	2.0	5
53	Slippage in stacking of graphene nanofragments induced by spin polarization. Scientific Reports, 2015, 5, 10985.	3.3	9
54	Charging-induced asymmetric spin distribution in an asymmetric (9,0) carbon nanotube. Physical Chemistry Chemical Physics, 2015, 17, 28860-28865.	2.8	6

#	Article	IF	CITATIONS
55	U@C ₂₈ : the electronic structure induced by the 32-electron principle. Physical Chemistry Chemical Physics, 2015, 17, 23308-23311.	2.8	40
56	Structural and electronic properties of uranium-encapsulated Au14 cage. Scientific Reports, 2015, 4, 5862.	3.3	29
57	Environmental-Confinement-Induced Stability Enhancement of Chiral Molecules. ChemPhysChem, 2014, 15, 2672-2675.	2.1	0
58	The ground state and electronic structure of Gd@C82: A systematic theoretical investigation of first principle density functionals. Journal of Chemical Physics, 2014, 141, 244306.	3.0	22
59	Defect-induced strong localization of uranium dicarbide on the graphene surface. Physical Chemistry Chemical Physics, 2014, 16, 22784-22790.	2.8	16
60	Effect of ligands on the characteristics of (CdSe) ₁₃ quantum dots. RSC Advances, 2014, 4, 27146-27151.	3.6	23
61	De Novo Design of an Endohedral Heteronuclear Dimetallofullerene (UGd)@C ₆₀ with Exceptional Structural and Electronic Properties. ChemPhysChem, 2014, 15, 3871-3876.	2.1	10
62	Stable electronic structures of a defective uranofullerene. Carbon, 2014, 78, 19-25.	10.3	11
63	Carbon nanotubes adsorb U atoms differently in their inner and outer surfaces. RSC Advances, 2014, 4, 30074.	3.6	10
64	Basis set effect on defect induced spin polarization of a carbon nanotube in density functional theory calculations. Chemical Physics Letters, 2013, 585, 107-111.	2.6	4
65	Strong Adsorption Between Uranium Dicarbide and Graphene Surface Induced by f Electrons. Journal of Physical Chemistry C, 2013, 117, 26849-26857.	3.1	14
66	Defect Induced Electronic Structure of Uranofullerene. Scientific Reports, 2013, 3, 1341.	3.3	30
67	Energetics and Electronic Properties of a Neutral Diuranium Molecule Encapsulated in C90 Fullerene. Procedia Chemistry, 2012, 7, 528-533.	0.7	13